Nano World Journal

https://doi.org/10.17756/nwj.2023-s1-101

Research Article

Open Access

Investigating the Effect of Material Properties and Geometric Design of Scaled Magneto-rheological Brake through FEMM

Shubham Kadam, Ashok Kumar Kariganaur and Hemantha Kumar*

Department of Mechanical Engineering, National Institute of Technology Karnataka, Surathkal, Mangalore, Karnataka, India

***Correspondence to:**
Hemantha Kumar
Department of Mechanical Engineering,
National Institute of Technology Surathkal,
Mangalore, Karnataka, India.
E-mail: hemantha@nitk.edu.in

Received: November 24, 2022
Accepted: May 05, 2023
Published: May 07, 2023

Citation: Kadam S, Karignaur AK, Kumar H. 2023. Investigating the Effect of Material Properties and Geometric Design of Scaled Magneto-rheological Brake through FEMM. *NanoWorld J* 9(S1): S523-S528.

Copyright: © 2023 Kadam et al. This is an Open Access article distributed under the terms of the Creative Commons Attribution 4.0 International License (CCBY) (http://creativecommons.org/licenses/by/4.0/) which permits commercial use, including reproduction, adaptation, and distribution of the article provided the original author and source are credited.

Published by United Scientific Group

Abstract

Magneto-rheological (MR) brakes have enormous potential to replace conventional brakes because of their higher degree of controlling capability. With the help of magnetic field, MR brakes can be activated to provide braking. Appropriate material selection and geometric dimensions will maximize MR brakes' performance. The present study focuses on determining higher magnetic permeable material to generate more magnetic induction in the fluid gap, along with finding geometric dimensions of the scaled (miniature sized) MR brakes (mass <2kg) through finite element analysis. Finite Element Method Magnetics (FEMM) software is a helpful tool for determining magnetic induction present in the MR gap. The influence of several magnetic and non-magnetic materials on disc-type MR brakes is examined. MR brake's geometric dimensions significantly influence the magnetic induction in the fluid-filled MR gap, and the ideal material combination necessary for improved performance is identified. The geometric dimensions were selected by varying fluid gaps between 1 - 3 mm and rotor radius of 15 mm and 30 mm. The study examined two plate MR brake performance in the outer and inner MR fluid gaps using optimal materials and geometric dimensions obtained from the initial sections.

Keywords

Magnetorheological fluids, Magnetorheological brakes, Finite element method magnetics analysis, Magnetic induction

Introduction

MR fluids are a class of intelligent materials that can change their flow properties with an external magnetic field supply. MR fluids consist of ferromagnetic particles such as carbonyl iron, additives such as bentonite, and clay suspended in carrier oils such as silicon oil. Without a magnetic field, MR fluids behave as Newtonian fluids. However, when a magnetic field is introduced, the existing ferromagnetic particles orient themselves along the magnetic field lines. This behaviour change can be controlled; hence, it has been utilized in many applications, including dampers, clutches, brakes, mounts, valves, etc. A quasi-static, one-dimensional model can be successfully used to understand the magnetic properties of MR fluids. A model can show the magnetic induction distribution within the MR fluid and how the magnetic induction varies as the saturation is approached due to an increase in field intensity [1, 2]. Depending on shear stress values, MR fluids can be grouped into before yield and after yield regions. Under the pre yield region, MR fluids exhibit viscoelastic properties, which can be used in different applications. Using MR fluid as a control medium for brake systems, one can find that torque transmitted increases with the intensifying magnetic field, and finite element analysis can be used to model a strong electromagnet [3, 4]. An automotive MR brake was typically modeled

and studied for design dimensions and heat generation around the brake using finite element analysis [5]. Researchers have shown that the power law technique can be used to obtain performance, and new magnetic circuits can be designed. It is shown that space constraints can be obtained by using various fit equations [6, 7]. Temperature increase within the brake can be significantly reduced by employing water cooling around the system, enhancing the MR brake's performance [8]. Minimizing the unnecessary material interruption to decrease the magnetic flux length, the MR brake performance can be improved significantly [9]. Alternating the core design and composition of the MR brake rotor with magnetic and non-magnetic material has a significant impact on the performance of the brake and provides lesser flux leakage focusing the magnetic field on the rotor periphery [10, 11]. MR brakes can replace conventional hydraulic brakes by optimizing the design parameters of MR brakes through the finite element method. MR brake for middle-sized passenger cars is possible through finite element analysis in a combination of a tool for optimal geometric dimensions. A T-shaped MR drum brake can also activate radial and axial magnetic flux around the MR brake system for increased motorcycles performance. Flow analysis can be performed numerically using the Navier-Stokes and Bingham non-linear model [12-15]. Using a mathematical model of an MR Brake, higher torques can be achieved by keeping the system weight low using a genetic algorithm [16]. MR Brake with high torque transmission capacity can be achieved using double shearing discs and optimizing the magnetic field. For dual brake discs, by utilizing non-magnetic sleeves, the magnetic field lines can be guided better throughout the MR brake system [17, 18]. Overall, the literature concentrates on design and MR brake using FEMM analysis. However, a comprehensive study on the design of miniature-sized MR brakes is needed. Hence, this study is concentrated on MR brake design of reduced size. The following sections examine the impact of adjusting various geometric design factors on the field strength in the MR gap area and dual plate MR brake study.

Materials and Methods

Methodology

The methodology flowchart shown in figure 1; initially deals with finding magnetic and non-magnetic materials for efficient magnetic induction inside the MR gap. Material selection considers factors like weight density and magnetic induction at saturation. The next stage obtains the magnetic induction values for changes in different geometric parameters like rotor radius, MR gap variation, etc. The last step involves modeling a two-plate MR brake that utilizes optimum material and dimensions for higher magnetic induction.

MR brake configuration

MR Brake is an amalgamation of magnetic and non-magnetic materials. Non-magnetic materials have low magnetic permeabilities, resulting in more resistance to conveying magnetic induction lines through the system. Magnetic materials have high magnetic permeabilities, resulting in higher conductance to carry magnetic induction lines. The primary objective of the MR brake system is to concentrate all the induction lines in the MR fluid-filled gap. The magnetic induction lines are not desired to flow beyond the MR fluid gap. Figure 2 represents an ideal MR brake configuration with different components and material types.

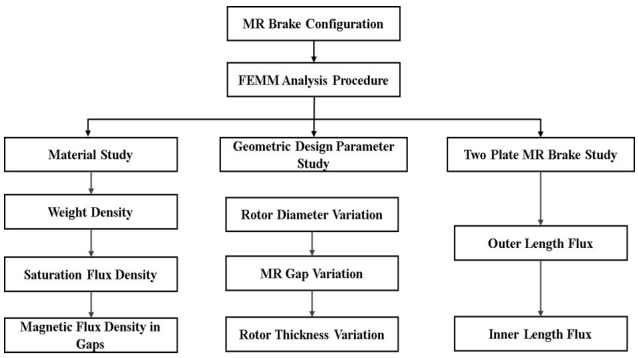


Figure 1: Methodology adopted.

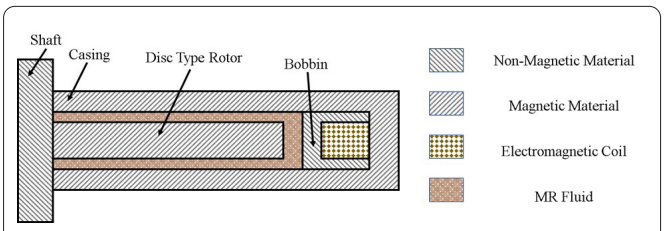


Figure 2: Disc type MR brake configuration.

FEMM analysis procedure

This study involves a 2-D analysis of a FEMM-created MR brake model. Materials are added to each section from the FEMM materials library. Modeling of MR braking device is performed, including magnetic circuit design based on magnetic Kirchhoff's rules.

$$\sum Hl = NI \tag{1}$$

Where, H is the magnetic field intensity of the circuit, N is the number of coil turns, and l is the overall effective length. For a single-rotor MR brake, the effective length is given as:

$$l = 2g \tag{2}$$

Where, g is the MR gap length of each shearing area.

At low magnetic fields, the magnetic induction (B) increase in proportion to the magnetic field intensity (H) as follows:

$$B = \mu_o \mu_r H \tag{3}$$

Where, μ_o is the magnetic permeability of free space ($4\pi 10^{-7}$ Tm/A) and μ_r is the relative permeability of the material.

Thus, from equation (1) and (2), the magnetic field intensity in the MR gap can be written as [19]:

$$H_{MR} = \frac{NI}{2g} \tag{4}$$

Similarly, incorporating equation (4) in equation (3) we get magnetic induction as:

$$B = \frac{\mu_{ii}\mu \quad NI}{2g} \tag{5}$$

Where, μ_{MR} is the relative magnetic permeability of MR fluid. Through equation (5), the number of turns incorporated in the FEMM MR brake model is found by assuming values given in table 1.

Table 1: Parameters considered for FEMM Analysis.

Parameter	Values
Magnetic Induction (*B*)	0.5 T
Relative permeability of MR fluid (μ_{MR})	5
Current (*I*)	1 A
Fluid Gap Length (*g*)	1 mm

The approximate number of coil turns was determined to be 300. As an electromagnetic coil, 26 AWG copper wire was considered; default mesh size and Dirichlet boundary conditions were employed throughout the analysis. Incorporating Dirichlet boundary conditions assures that no magnetic induction flows out of the boundary. Figure 3b depicts a meshed model of a FEMM MR brake. The MRF-132DG B-H curve values were determined using a rheometer. These values were input in FEMM to define a new material that is assigned to the MR fluid gap in the model. Figure 3a illustrates the B-H curve of MRF-132DG.

Results and Discussion

The effectiveness of the MR brake is dependent on the permeability of the materials used in its construction, the fluid gap, and the number of rotors. The study is discussed in the steps listed below.

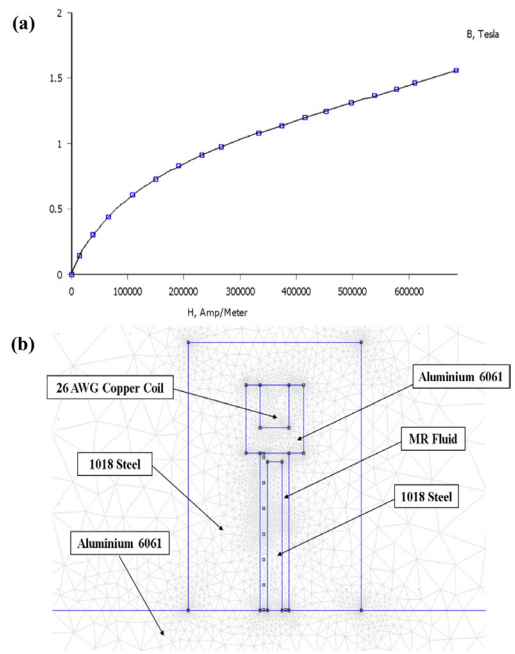


Figure 3: (a) MRF 132 DG B-H curve and **(b)** FEMM meshed model.

Material selection study

All the materials considered in the study are available from the FEMM material library. Table 2 present the mass density of non-magnetic and magnetic substances. Non-magnetic materials aid in keeping induction lines beneath MR gap; hence, a lightweight material with good strength is favoured. Magnetic materials follow a thorough selection procedure. In this study, each magnetic material is independently maintained as a stator by maintaining a constant 1018-steel rotor. The maximum magnetic induction in the MR gap is then determined by analyzing each combination through FEMM for maximum current (3 A). The values are displayed in table 3. Any substance that exceeds the induction value above saturation induction is excluded from further examination.

Material variation study

From table 2 and table 3, it can be observed that 1018, 1020 Steels, and iron have higher saturation induction and gives better maximum magnetic induction values with similar weight density. All three magnetic materials are used as rotors, and the performance of each one for different stator materials has been plotted using the contour described in figure 4a. From figure 4b, 4c, and 4d, it can be noticed that Hiperco-50, as a stator, gives the highest magnetic induction values in the MR gap. But it has the highest weight density among the magnetic materials. This study prefers maintaining a lower-weight system. Hence lower weight density materials for stators are utilized for further analysis. Iron, 1020 Steel, and 1018 Steel show higher to average magnetic induction values, respectively. Hence, preference should be given to these materials for MR brake construction. The material selection and variation studies indicate that Iron and 1020 steel can be used as rotor and stator for higher MR brake performance. Hence, the further geometric study will be carried out with 1020 steel as rotor-stator material.

Table 2: Density of Non-Magnetic Materials and Magnetic Materials.

Type	Material	Density (Kg/m3)
Non-Magnetic	316 Stainless Steel	7980
	Aluminium 6061 Alloy	2700
	Copper	8960
Magnetic	1018 Steel	7870
	1020 Steel	7870
	Iron	7870
	M19 Steel	7650
	M45 Steel	7650
	Hiperco-50	8120
	455 Stainless Steel	7800
	430 Stainless Steel	7800
	Mu Metal	8800
	Supermalloy	7874

Table 3: Comparison of saturation and maximum magnetic induction of magnetic materials.

Casing Material	1018 Steel	1020 Steel	Iron	Hiperco-50	430 SS	455 SS	M19 Steel	M45 Steel	Mu Metal	Supermalloy
Maximum Induction	2.077	2.253	2.183	2.25	1.7	1.638	2.03	2.083	0.822	3.11
Saturation Induction	2.43	2.579	2.56	2.341	2.08	1.5	2.3	2.3	0.662	0.785
Acceptable/ Unacceptable	✓	✓	✓	✓	✓	✗	✓	✓	✗	✗

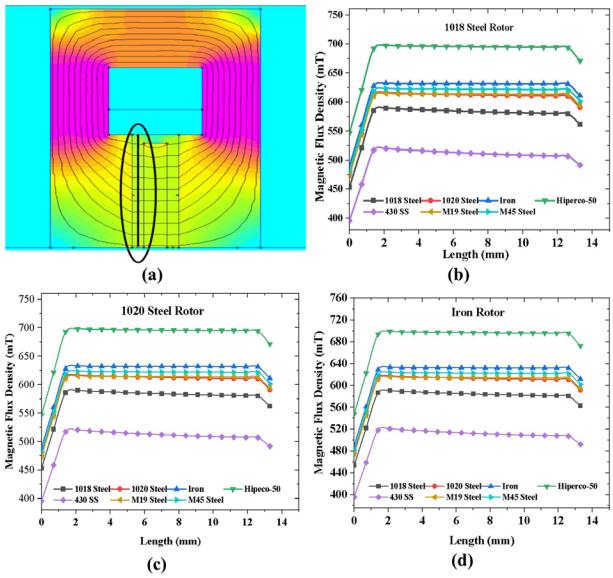


Figure 4: (a) Contour length in MR fluid gap to plot Magnetic Induction Variation; **(b)** Magnetic Induction Variation for 1018 Steel; **(c)** Magnetic Induction Variation for 1020 Steel; and **(d)** Magnetic Induction Variation for Iron.

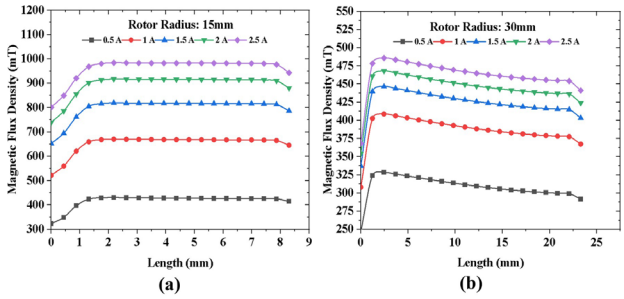


Figure 5: Current Variation Effect on Magnetic Induction for **(a)** 15 mm and **(b)** 30 mm rotor radius.

Geometric variation study

Magnetic Induction Variation for rotor radius of 15 mm, and 30 mm on the application of different currents can be observed in figure 5a and 5b. It shows that the increment of rotor radius leads to a higher decreasing slope of magnetic induction values, indicating that the selection of rotor radius is essential to achieve the required braking performance. Hence, the rotor radius must be selected effectively. MR fluid gap width is an important parameter. Increasing the MR gap would result in the inefficient stacking of ferromagnetic particles within the gap when a current is applied. Consequently, MR gap variations relative to the contour are exhibited for various rotor diameters 15 mm and 30 mm in figure 6a and 6b. There is approximately 150% more induction at the lower fluid gap (1 mm) than at, the higher (3 mm). Hence, a lower gap selection (preferably 1 mm) would be appropriate to construct an MR brake without increasing manufacturing complexity. On similar lines, increased rotor thickness may result in more magnetic flux lines drawn through the rotors, which is evident in figure 7. The average magnetic induction for rotors with a thickness of 3 mm is marginally greater. As shown in the figure, an increase in rotor thickness slightly increases the maximum induction and the system weight. The present study concentrates on disc-type MR brakes; higher rotor dimensions will classify into drum-type MR brakes where braking torque is significantly achieved through radial gaps. Hence, rotor thickness must be selected to obtain appreciable magnetic induction in the axial MR fluid gaps.

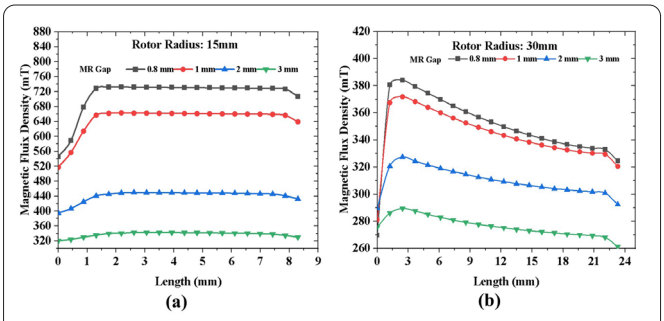


Figure 6: MR fluid gap variation effect on Magnetic Induction for **(a)** 15 mm and **(b)** 30 mm rotor radius.

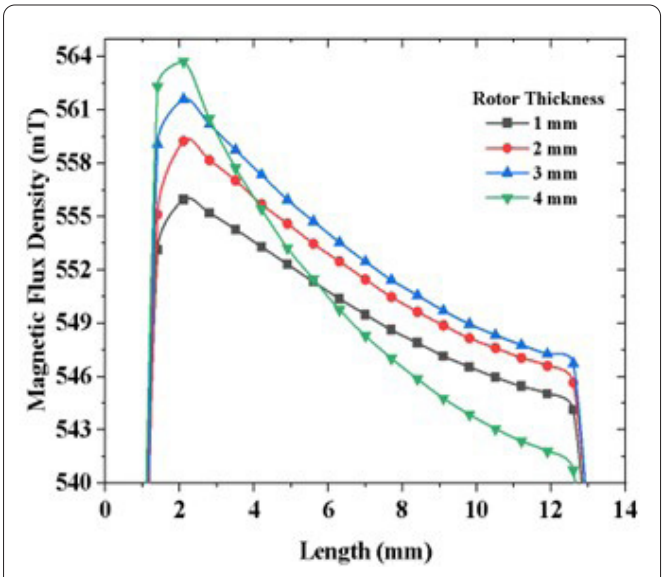


Figure 7: Rotor Thickness Variation on Magnetic Induction.

Single-rotor MR brake has only two shearing areas to provide the braking torque. The more shearing areas, the higher will be the torque produced. Single-rotor MR brake needs higher dimensions and weight for higher torque applications. Hence, a preliminary study showing a FEMM analysis of a two-plate MR brake is displayed in figure 8. Two plate MR brake has four shearing areas, leading to better torque output without compromising systems dimensions and weight. The magnetic induction variation in the inner and outer MR gap is also displayed in figure 8. It is important to note that the magnetic induction intensity decreases slightly as we move toward internal fluid gaps. The average magnetic induction values between the single-rotor and two-rotor MR brake are 700 mT and 500 mT, respectively. But since the shearing areas are more in later, it will achieve higher braking torque. Thus, multi-plate MR brakes can help achieve high braking torques.

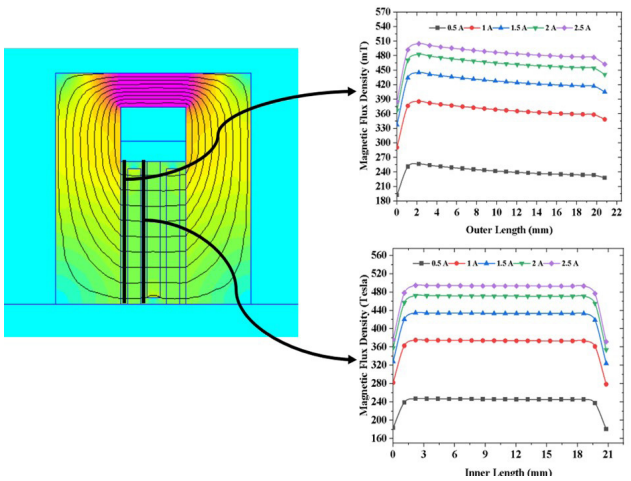


Figure 8: Two-plate MR brake Magnetic Induction Plots for inner and outer.

Conclusions

The study aims to find the optimum material and geometric parameters of an MR brake. Material with higher magnetic permeability increases magnetic induction by approximately 30 - 40% in the fluid gap. It is evaluated from the results that low fluid gaps and a comparable rotor radius can increase torque generation. Finally, increasing the number of rotors will increase the torque generation, which depends on the requirement of suitable applications. The entire miniature-sized MR brake study with material selection, design, and geometric parameters will aid in different applications like assistive knee braces, wrist rehabilitation devices, etc.

Acknowledgments

The author(s) disclosed receipt of the following financial support for the research, authorship, and/or publication of this article: This work was supported by the Department of Science and Technology, Government of India [Project No. SEED/TIDE/2019/644/G]. The project's title is "Design and Development of Semi-active prosthetic knee using cost-effective magnetorheological (MR) brake to assist trans-femoral amputees."

Conflict of Interest

The authors declare no conflict of interests that are relevant to the content of this article.

Credit Author Statement

Shubham Kadam: Conceptualization, Methodology, Formal analysis, Investigation, Writing - original draft preparation; Ashok Kumar Kariganaur: Conceptualization, Methodology, Writing - original draft preparation; Hemantha Kumar: Writing - review and editing, Resources, Supervision. All the authors read and approved the manuscript.

References

1. Jolly MR, Carlson JD, Munoz BC. 1996. A model of the behaviour of magnetorheological materials. *Smart Mater Struct* 5(5): 607. https://doi.org/10.1088/0964-1726/5/5/009
2. Jolly MR, Bender JW, Carlson JD. 1999. Properties and applications of commercial magnetorheological fluids. *J Intell Mater Syst Struct* 10(1): 5-13. https://doi.org/10.1177/1045389X9901000102
3. Li WH, Chen G, Yeo SH. 1999. Viscoelastic properties of MR fluids. *Smart Mater Struct* 8(4): 460. https://doi.org/10.1088/0964-1726/8/4/303
4. Li WH, Du H. 2003. Design and experimental evaluation of a magnetorheological brake. *Int J Adv Manuf Technol* 21: 508-515. https://doi.org/10.1007/s001700300060
5. Karakoc K, Park EJ, Suleman A. 2008. Design considerations for an automotive magnetorheological brake. *Mechatronics* 18(8): 434-447. https://doi.org/10.1016/j.mechatronics.2008.02.003
6. Yu L, Ma L, Song J. 2017. Design, testing and analysis of a novel automotive magnetorheological braking system. *Proc Inst Mech Eng D J Automob Eng* 231(10): 1402-1413. https://doi.org/10.1177/0954407016674394
7. Lijesh KP, Kumar D, Gangadharan KV. 2018. Design of magneto-rheological brake for optimum dimension. *J Braz Soc Mech Sci Eng* 40(3): 161. https://doi.org/10.1007/s40430-018-1089-5
8. Wang DM, Hou YF, Tian ZZ. 2013. A novel high-torque magnetorheological brake with a water cooling method for heat dissipation. *Smart Mater Struct* 22(2): 025019. https://doi.org/10.1088/0964-1726/22/2/025019
9. Nam YJ, Moon YJ, Park MK. 2008. Performance improvement of a rotary MR fluid actuator based on electromagnetic design. *J Intell Mater Syst Struct* 19(6): 695-705. https://doi.org/10.1177/1045389X07079463
10. Sohn JW, Gang HG, Choi SB. 2018. An experimental study on torque characteristics of magnetorheological brake with modified magnetic core shape. *Adv Mech Eng* 10(1): 1687814017752222. https://doi.org/10.1177/1687814017752222
11. Acharya S, Kumar H. 2019. Investigation of magnetorheological brake with rotor of combined magnetic and non-magnetic materials. *SN Appl Sci* 1: 1-7. https://doi.org/10.1007/s42452-019-1029-8
12. Nguyen QH, Choi SB. 2010. Optimal design of an automotive magnetorheological brake considering geometric dimensions and zero-field friction heat. *Smart Mater Struct* 19(11): 115024. https://doi.org/10.1088/0964-1726/19/11/115024
13. Nguyen QH, Choi SB. 2012. Optimal design of a novel hybrid MR brake for motorcycles considering axial and radial magnetic flux. *Smart Mater Struct* 21(5): 055003. https://doi.org/10.1088/0964-1726/21/5/055003
14. Nguyen QH, Choi SB. 2011. Selection of magnetorheological brake types via optimal design considering maximum torque and constrained volume. *Smart Mater Struct* 21(1): 015012. https://doi.org/10.1088/0964-1726/21/1/015012

15. Attia EM, Elsodany NM, El-Gamal HA, Elgohary MA. 2017. Theoretical and experimental study of magneto-rheological fluid disc brake. *Alexandria Eng J* 56(2): 189-200. https://doi.org/10.1016/j.aej.2016.11.017

16. Assadsangabi B, Daneshmand F, Vahdati N, Eghtesad M, Bazargan-Lari Y. 2011. Optimization and design of disk-type MR brakes. *Int J Automot Technol* 12: 921-932. https://doi.org/10.1007/s12239-011-0105-x

17. Zhou W, Chew CM, Hong GS. 2007. Development of a compact double-disk magneto-rheological fluid brake. *Robotica* 25(4): 493-500. https://doi.org/10.1017/S0263574707003372

18. Hu G, Wu L, Li L. 2021. Torque characteristics analysis of a magnetorheological brake with double brake disc. *Actuators* 10(2): 23. https://doi.org/10.3390/act10020023

19. Krishna H, Kumar H, Gangadharan K. 2017. Optimization of magneto-rheological damper for maximizing magnetic flux density in the fluid flow gap through FEA and GA approaches. *J Inst Eng India Ser C* 98: 533-539. https://doi.org/10.1007/s40032-016-0251-z